Oxide Film Formation and Oxygen Adsorption on Copper in Aqueous Media As Probed by Surface-Enhanced Raman Spectroscopy

Ho Yeung H. Chan,[†] Christos G. Takoudis,[‡] and Michael J. Weaver*[,§]

School of Chemical Engineering and Department of Chemistry, Purdue University, West Lafayette, Indiana 47907, and Department of Chemical Engineering, University of Illinois at Chicago, Chicago, Illinois 60607

Received: September 21, 1998; In Final Form: November 12, 1998

The electrode potential-dependent formation of oxygen species on copper in noncomplexing aqueous media, encompassing oxide phase films and adsorbed oxygen/hydroxide, are explored at different pH values by means of surface-enhanced Raman spectroscopy (SERS). This technique provides a monolayer-sensitive in-situ vibrational probe, which can follow potential-dependent surface speciation on voltammetric or longer time scales. In alkaline $NaClO_4$ electrolytes (pH 13), the cyclic voltammetric peaks associated with copper oxide phase-film formation and removal are correlated quantitatively with simultaneously acquired SER spectral sequences. The latter indicate the sequential formation of Cu_2O and then mixed $Cu_2O/Cu(OH)_2$ layers, diagnosed by the appearance of metal−oxygen lattice vibrations at 625/525 and 460 cm^{-1}, respectively. The potential-dependent speciation is in concordance with the Pourbaix diagram, certifying the "bulk-phase" nature of the films. The Raman band intensity−film thickness correlation (the latter deduced from the voltammetric Coulombic charges) indicate that the vibrational spectral responses are limited to the first 15−20 monolayers, consistent with earlier SERS observations and theoretical predictions. Weaker bands at ca. 800 and 460 cm^{-1} are discernible at more negative potentials, suggestive of hydroxide adsorption. Similar, although thinner, oxide films were deduced to form in neutral 0.1 M $NaClO_4$. In the additional presence of chloride under these conditions, a potential-sensitive competition between the formation of a CuCl and a more passivating Cu_2O phase film was evident from SERS. While oxide phase films are absent on copper in 0.1 M H_2SO_4 and 0.1 M $HClO_4$, an adsorbed oxygen species was nonetheless detected from a broad SERS band at ca. 625 cm^{-1}. This feature, which was deduced to involve oxygen rather than hydroxyl from an absence of a frequency shift upon H/D solvent isotopic substitution, is evident throughout most of the "polarizable potential" region on copper in acid, ca. −0.7 to −0.1 V vs SCE. The likely nature and reasons for its remarkable prevalence on copper in acidic media are discussed with reference to the recent literature.

Introduction

Elucidating the nature and occurrence of copper surface oxidation in aqueous solution-related ambient environments has long been sought, prompted by the high affinity of this metal for oxygen and its multifaceted practical significance. A key issue for which fundamental understanding remains inadequate concerns the electrode potential-dependent formation of adsorbed oxygen and surface oxide species in aqueous media of varying pH. While information along these lines can be obtained by means of conventional electrochemical measurements, it is clearly desirable to acquire chemically specific information regarding the metal surface composition by means of molecular and other spectroscopies. Indeed, X-ray photoelectron spectroscopy (XPS) performed on emersed copper electrodes has been utilized to identify the nature of copper oxide films formed in alkaline and neutral solution.[1] It is advantageous, however, to utilize in-situ spectroscopic methods in that electrode emersion tactics can yield ambiguous results, especially since reversibly adsorbed species are often removed or altered under these conditions.

Vibrational spectral techniques are of particular value given their sensitivity to adsorbate structure and bonding. While both in-situ Raman[2] and infrared[3] spectroscopies have been utilized previously to examine copper electrooxidation in alkaline media, the strategies employed did not achieve monolayer sensitivity, vibrational spectra only for relatively thick films being obtained. As is well known, surface-enhanced Raman spectroscopy (SERS) offers sufficient sensitivity for this purpose even at the lower wavenumbers (<800 cm^{-1}) where metal−oxygen vibrations are commonly located, and copper is an intrinsically SERS-active metal. Numerous SERS studies have been reported on copper, especially involving organic adsorbates. However, fundamental examinations of copper oxidation by this means are conspicuous by their absence, even though an interesting recent SERS study on mildly roughened Cu(111) provides evidence of hydroxide adsorption at far negative potentials in concentrated alkaline solution.[4] The Purdue group has employed SERS previously to examine the electrooxidation of gold and Pt-group transition-metal surfaces,[5−7] and oxidation of the latter also in elevated-temperature gaseous environments.[8] (The transition metals are prepared by thin-film electrodeposition on SERS-active gold.[6,9]) These and related studies[10] have demonstrated the value of SERS to ascertain the nature of oxide films having thicknesses down to monolayer levels.

* Corresponding author. Tel: (765) 494-5466. Fax: (765) 494-0239. E-mail: mweaver@purdue.edu.
[†] School of Chemical Engineering, Purdue University.
[‡] Department of Chemical Engineering, University of Illinois at Chicago.
[§] Department of Chemistry, Purdue University.

10.1021/jp983787c CCC: $18.00
Published on Web 12/29/1998

The study reported herein utilizes SERS to investigate the surface structural changes associated with the potential-dependent oxidation and reduction of copper in alkaline, neutral, and acidic media. As in our previous electrochemical SERS studies of this type, real-time Raman spectral sequences are obtained partly in conjunction with cyclic voltammetric data so to identify the surface compositional changes responsible for specific current−potential features. Multilayer surface oxidation in alkaline media is examined first in view of the previous work along these lines mentioned above, together with the presence of voltammetrically well-defined oxidation/reduction steps. The competitive formation of Cu_2O and CuCl films is scrutinized in neutral chloride media given the competitive nature of these processes under these conditions. Lastly, the species likely to be present on copper electrodes in chloride-free acidic electrolytes are examined by SERS. Significantly, adsorbed oxygen species are deduced by SERS to be present even at electrode potentials which are substantially below those corresponding to multilayer oxide formation. These findings are compared with recent evidence for adsorbed oxygen on copper electrodes as gleaned from in-situ atomic force microscopy (AFM).[11]

Experimental Section

Most details of the experimental setup used for electrochemical SERS are given in ref 12. Briefly, a Spectra Physics Stabilite (Model 2017) Kr^+ laser provides the Raman excitation at 647.1 nm with ca. 30 mW incident power on the electrode surface. Scattered light was collected via a camera lens into a SPEX (Model 1877) Triplemate Spectrometer, equipped with a Photometrics CCD detector. The in-situ SERS measurements utilized a standard three-electrode electrochemical cell with a quartz base window through which the laser beam was incident on the copper surface. The copper electrode, having an exposed area of 0.12 cm^2, is sheathed with Teflon, and a platinum wire is used as the counter electrode. Following mechanical polishing with 0.3 μm alumina, the copper electrode was mildly roughened by electrochemical oxidation−reduction cycles (ORC) in 0.1 M KCl[20] to generate a SERS-active surface. An ORC procedure yielding stable as well as intense SERS involves a potential sweep at 100 mV s^{-1} from −1.0 to 0.4 V, holding for 1 s, and sweeping back to −1.0 V at 100 mV s^{-1}, holding for 10 s before the next cycle. A total of 15 cycles were typically used. The electrode was then emersed at −1.0 V, rinsed with deionized water to remove residual chloride, and transferred to the SERS cell. The XPS experiments, utilizing a Perkin−Elmer PHI 5300 instrument, were performed on copper foils (0.13 mm thick) that were also prepared and characterized by the above means by mounting on a Teflon-sheathed sample holder.

The sulfuric acid and perchloric acid electrolytes were prepared from ultrapure reagents (double-distilled grade, GFS Chemicals). Sodium perchlorate was reagent grade (GFS Chemicals) and sodium hydroxide was ultrapure (Alfa). Solutions were prepared from water purified by a Milli Q system (Millipore). The electrode potentials were measured and are quoted with respect to the saturated calomel electrode (SCE).

Results and Discussion

Alkaline Media. It is instructive to consider first voltammetric oxidation, along with simultaneously acquired SER spectra of the copper surface in alkaline media given the detailed electrochemical and spectroscopic characterization[1−3] that is already available under these conditions. Figure 1 shows a pair of typical anodic−cathodic cyclic voltammograms for SERS-active copper in 0.1 M $NaClO_4$ + 0.1 M NaOH (pH 13). The

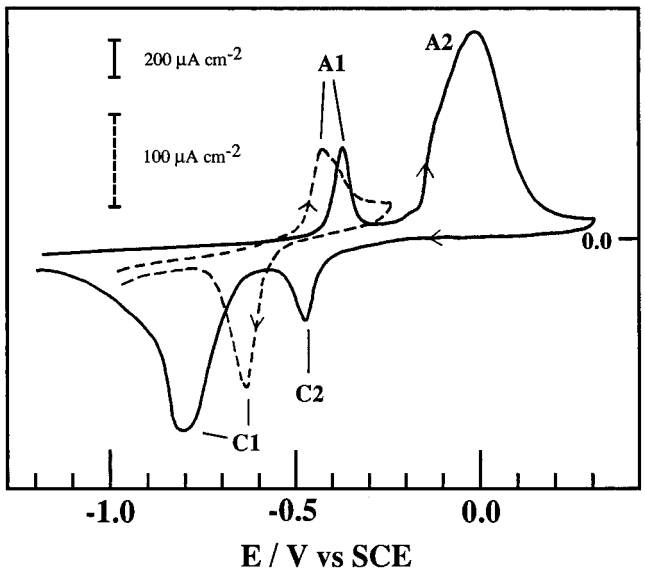

Figure 1. Typical cyclic voltammograms for copper in 0.1 M NaOH + 0.1 M $NaClO_4$ (pH 13) at 5 mV s^{-1} (solid trace) and 1 mV s^{-1} (dashed trace).

solid trace, obtained at 5 mV s^{-1}, spans a potential region from −1.2 to 0.3 V and return, which encompasses two anodic peaks (A1 and A2) and the accompanying cathodic features (C2 and C1). The dashed trace, at 1 mV s^{-1}, utilizes a reversal potential, −0.25 V, so that only the more negative potential features (A1, C1) are accessed. It is known that the anodic peak A1 arises from the oxidation of Cu to yield a multilayer Cu_2O film, and A2 is associated with the formation of $Cu(OH)_2$ along with the further production of Cu_2O,[1−3] according to:

$$2Cu + H_2O \leftrightarrow Cu_2O + 2H^+ + 2e^- \quad (1a)$$

$$Cu_2O + 3H_2O \leftrightarrow 2Cu(OH)_2 + 2H^+ + 2e^- \quad (1b)$$

The reduction of $Cu(OH)_2$ to Cu_2O is responsible for C2 and followed by the final reduction of Cu_2O back to Cu (wave C1). According to the Pourbaix diagram,[13] the equilibrium potential for Cu/Cu_2O, $E°_{(Cu_2O)}$, is −0.54 V vs SCE at pH 13, which lies between the potentials for A1 and C1 observed here (dashed trace, Figure 1). The hysteresis observed between A1 and C1 is expected given the well-known kinetic limitations of the oxide film formation and removal processes. The potential separation between A1 and C1 diminishes toward decreasing sweep rates so as to approach $E°_{(Cu_2O)}$, confirming the correspondence of these voltammetric features with the thermodynamics of "bulk-phase" Cu_2O formation.

Potential-dependent SER spectra obtained simultaneously with the 5 mV s^{-1} cyclic voltammogram (solid trace, Figure 1) are shown in Figures 2A and 2B, the former being acquired during the initial anodic sweep and the latter during the ensuing cathodic sweep. Given that the spectral acquisition time was 10 s, each spectrum shown in Figure 2A,B corresponds to an electrode potential increment of 50 mV. Only selected spectra are shown for clarity; the potentials indicated in Figure 2 refer to the average values during each data acquisition. (Note that the spectra are stacked upward with increasing time during the anodic−cathodic voltammogram in both figures.)

It is evident from Figure 2A that a broad SERS feature at 625 cm^{-1} along with a shoulder at 525 cm^{-1} appears by −0.38 V during the anodic sweep, corresponding to A1. Significantly, these spectral features did not exhibit frequency shifts ($\leq$5 cm^{-1})

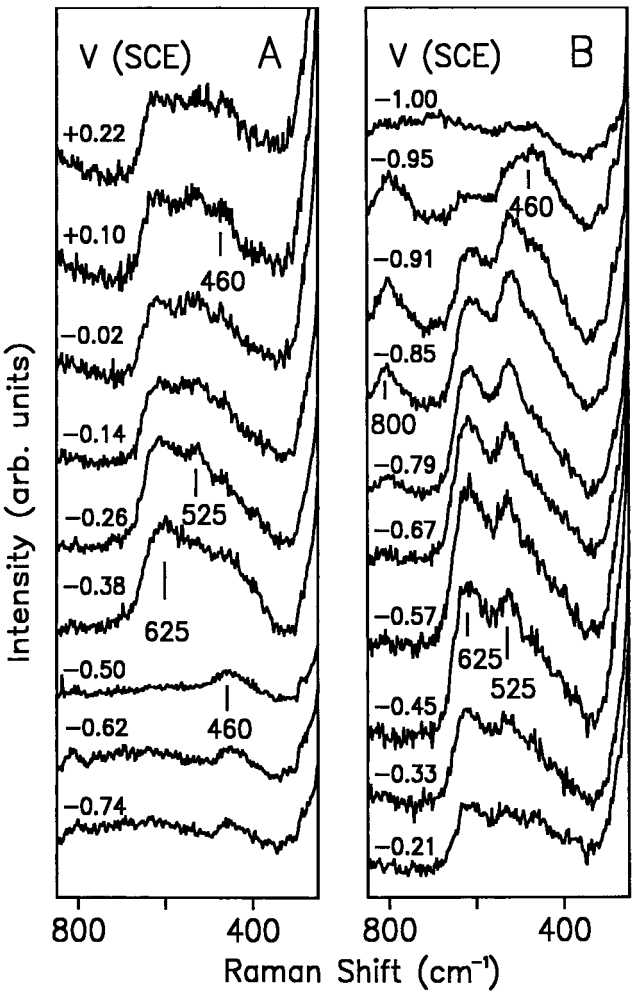

Figure 2. Selected real-time potential-dependent SER spectra for copper during (A) voltammetric oxidation and (B) subsequent reduction in 0.1 M NaOH + 0.1 M $NaClO_4$ at 5 mV s^{-1}, obtained simultaneously with the CV (solid trace) in Figure 1. The indicated potentials are the average values during each 10 s spectral acquisition period.

upon substitution of the aqueous solvent by D_2O. Since a ca. 20 cm^{-1} redshift upon deuteration is anticipated to occur if the vibration involves an −OH (−OD) species,[5,7] this finding is consistent instead with a Cu−O vibrational assignment. To identify the in situ SER spectra with specific oxides present in the thin film, it is useful to inspect the normal Raman spectra of different bulk-phase copper oxides.[2a] Both bulk CuO and Cu_2O exhibit a major Raman feature at ca. 635 cm^{-1}, whereas $Cu(OH)_2$ yields a band at 490 cm^{-1}. A distinction between CuO and Cu_2O can in principle be made by the presence of two minor Raman features at 490 and 410 cm^{-1} in the bulk-phase spectrum of the latter but not in the former. Therefore, the presence of the shoulder at 525 cm^{-1} along with the major 625 cm^{-1} band in the SER spectrum obtained during the initial oxidation step A1 is consistent with the formation of Cu_2O. (One should bear in mind, however, that the thin-film structure and even the stoichiometry may well differ from the corresponding bulk-phase species.) At higher potentials, in the vicinity of the second anodic peak A2 (at ca. 0 V), a weak additional SERS feature appears at 460 cm^{-1} (Figure 2A). This is tentatively assigned to $Cu(OH)_2$, again by comparison with bulk-phase Raman spectra.[2a]

It is interesting to compare the SERS results with literature reports of copper oxidation in basic media studied by in situ Raman[2] and infrared[3] spectroscopies. In particular, the Raman study by Hamilton et al.,[2a] using lower-wavelength (488 nm) laser excitation, reported that upon slow (1 mV s^{-1}) anodic voltammetric sweeps on copper in 0.1 M NaOH a Raman feature at 650 cm^{-1} was detected, but only at a higher potential than A1, 0.07 V, and a broad 500 cm^{-1} feature by 0.5 V. The former was assigned to Cu_2O and the latter to $Cu(OH)_2$ upon comparison with the bulk-phase oxide spectra. However, the potential-dependent appearance of the spectral bands for the oxide films did not correlate, at least on this time scale, with the corresponding voltammetric features. This complication appears to be due to the sensitivity limitations of the Raman strategy employed in ref 2a. Thus Cu_2O was detected only during the second voltammetric oxidation wave A2, evidently since the Cu_2O film thicknesses increases markedly at this stage in addition to $Cu(OH)_2$ formation. The detection limit of the Raman technique in ref 2a was examined by recording time-dependent Raman spectra after applying instead a potential step from −1.0 to −0.38 V (i.e., close to A1); Cu_2O Raman signals were only discernible after about 40 Å of oxide was grown.[2a] The discrepancy between the voltammetric and spectroscopic responses noted above is therefore clearly due to sensitivity restrictions. However, Hamilton et al. deduced clearly that their vibrational signals were due to resonant- rather than surface-enhanced Raman scattering by showing that no detectable spectra were obtained by altering the excitation wavelength from 488 to 647 nm.[2a] (Note that the former wavelength should incur resonant enhancement, at least for Cu_2O. As is well-known, obtaining intense SERS on copper requires excitation wavelengths above ca. 580 nm.[14]) A later Raman study, also using 488 nm excitation, of copper voltammetric oxidation in stronger base (1 and 6 M KOH)[2b] shows a closer correlation between the electrochemical and Raman results with respect to the onset of A1 and the emergence of the initially detectable Cu_2O Raman feature. This improved correspondence is probably due to more facile kinetics for copper oxidation at such higher pH values, so that the oxide is formed more rapidly, and hence more extensively, under voltammetric conditions.

A recent in-situ vibrational study of copper oxidation in alkaline media by Melendres et al. exploited the feasibility of acquiring sensitive far-infrared spectra by using a synchrotron light source.[3] The authors detected an infrared band at 630 cm^{-1} after cyclic voltammetric oxidation of Cu at −0.05 V in 0.1 M NaOH along with a 410 cm^{-1} band at 0.3 V, comparable to the 625 cm^{-1} and the 460 cm^{-1} SERS bands observed here. In harmony with the present interpretation, the former was assigned to Cu_2O and the latter tentatively assigned to CuO or $Cu(OH)_2$. Similarly to the Raman study in ref 2b, however, the authors of ref 3 did not detect the Cu_2O band in the proximity of A1, the oxide infrared signal only being discernible at potentials in the vicinity of A2.

In summary, these comparisons between the present SERS and earlier in-situ vibrational studies show concordance in the spectral features resulting from anodic copper oxidation. However, the greater sensitivity of SERS allows the clear assignment of A1 to Cu_2O formation, as well as A2 to combined Cu_2O and $Cu(OH)_2$ production. Besides vibrational studies, the oxidation of copper in alkaline media has also been investigated by XPS, identifying different copper oxidation states.[1] The ex-situ results support the present interpretation in that copper oxidizes to Cu_2O at A1, followed by further production of Cu_2O and $Cu(OH)_2$ during A2.

Turning now to the ensuing oxide electroreduction, Figure 2B shows selected SER spectra obtained during the return potential sweep, again obtained simultaneously with the CV shown in Figure 1 (solid trace). The 625 and 525 cm^{-1} bands

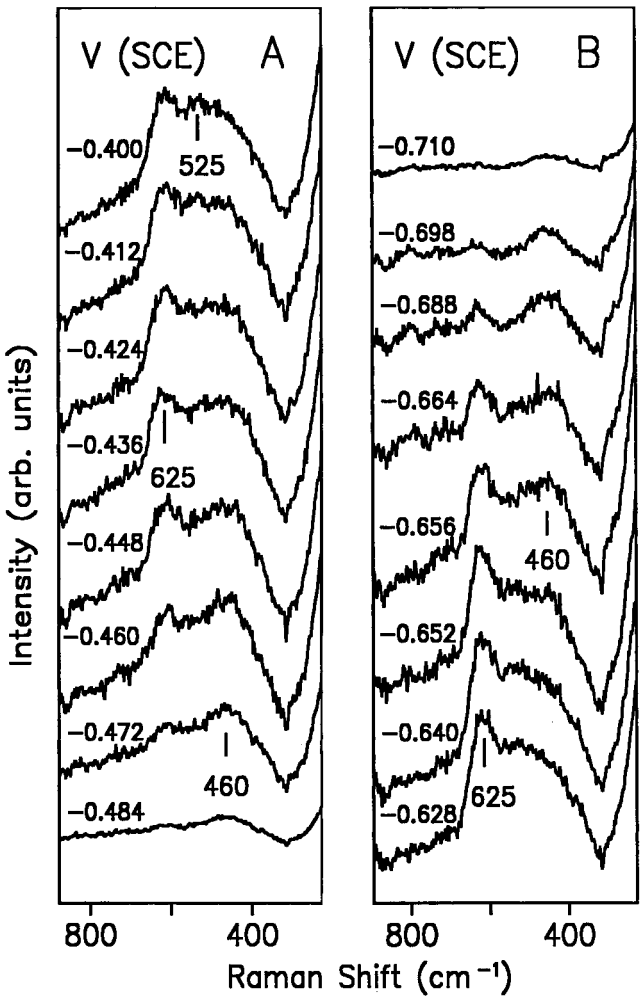

Figure 3. Selected real-time potential-dependent SER spectra for copper during (A) voltammetric oxidation and (B) subsequent reduction in 0.1 M NaOH + 0.1 M $NaClO_4$ at 1 mV s^{-1}, obtained simultaneously with the CV (dashed trace) in Figure 1. The indicated potentials are the average values during each 10 s spectral acquisition period.

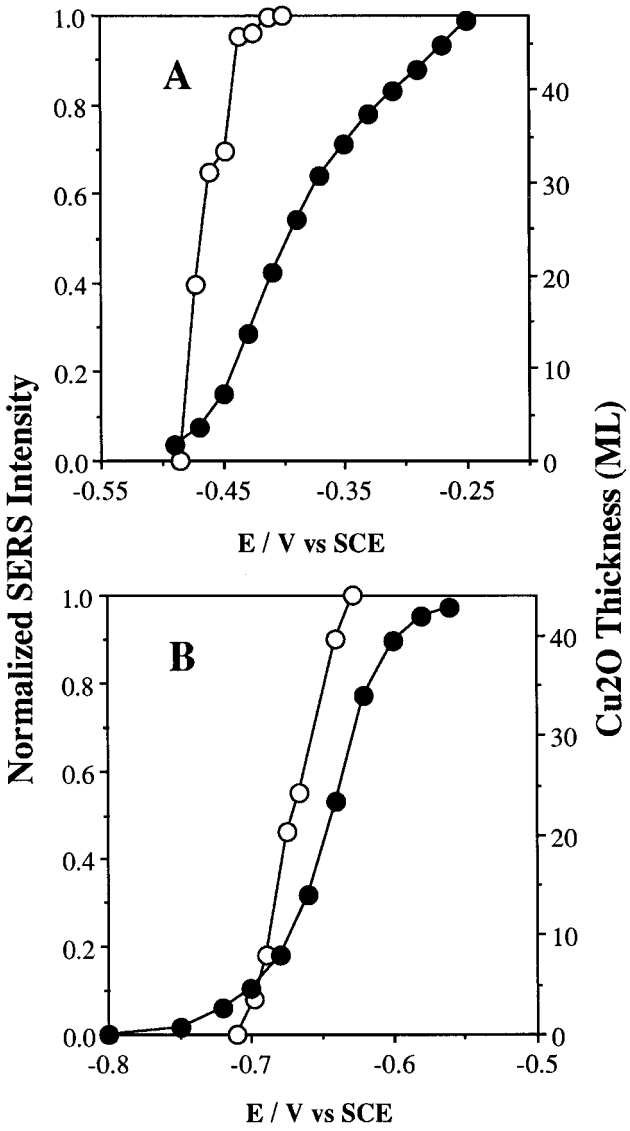

Figure 4. Plot of the normalized integrated SERS intensities for the Cu_2O band envelope (open circles) and oxide thickness (closed circles) versus electrode potential during (A) voltammetric oxidation and (B) subsequent reduction at 1 mV s^{-1} in 0.1 M NaOH + 0.1 M $NaClO_4$. Obtained from SERS and voltammetric data in Figures 3 and 1 (dashed trace), respectively.

are seen to become more pronounced at potentials, ca. −0.45 V, corresponding to the onset of C2. This is qualitatively reminiscent of the Raman results in both ref 2a and 2b, in which the 500 cm^{-1} band disappears during the negative-going sweep along with the reappearance of the Cu_2O Raman feature at 650 cm^{-1}, although, oddly, the spectral transformation occurs at a higher potential, ca. 0 V, than C2. Our SERS results, however, suggest that C2 is due to the reduction of $Cu(OH)_2$ to Cu_2O. Upon further lowering the potential to the location of C1, centered at −0.8 V, the observed attenuation of the 625/525 cm^{-1} bands (Figure 2B) signals a final reduction of Cu_2O to metallic copper. A band at 460 cm^{-1} also appears at this point (Figure 2B); a weaker 460 cm^{-1} feature is also evident at negative potentials prior to anodic oxide formation (Figure 2A). This band is plausibly assigned to adsorbed hydroxide (cf., SERS of gold electrodes in alkaline solution[5]). An 800 cm^{-1} SERS feature also appears at ca. −0.85 V during the negative-going sweep (Figure 2B). The 800 cm^{-1} as well as 460 cm^{-1} features are tentatively assigned to adsorbed hydroxide, specifically the Cu−OH bending and Cu−OH stretching modes, respectively, by comparison of vibrational spectra for oxygen/water adsorption on Cu(100) in ultrahigh vacuum (UHV)[15] (vide infra). The formation of the oxide films is accompanied by a substantial (ca. 3-fold) attenuation of the "continuum" SERS background signal, which is reversibly recovered upon oxide reduction. This phenomenon, however, is not understood at present.

Given that the appearance of the SERS 625/525 cm^{-1} features broadly correlates with the voltammetric formation and removal of Cu_2O, it is of interest to compare more closely the extent of surface oxidation and reduction as measured from the Coulombic charge for the A1 and C1 features with the corresponding potential-dependent Raman intensities obtained simultaneously. A slower sweep rate (1 mV s^{-1}) was chosen so to provide a better potential resolution for each spectrum (integration time 10 s, equivalent to 10 mV increments), with a lower reversal potential (−0.25 V) so to encompass only the first oxidation step, A1. The resulting potential-dependent SER spectra for copper in 0.1 M $NaClO_4$ + 0.1 M NaOH are displayed in Figure 3A (oxidation) and 3B (reduction) obtained simultaneously with the CV (Figure 1, dashed trace). Figure 4 shows the quantity of Cu_2O formed (in monolayers ML, filled circles) and the normalized integrated SERS intensity (open circles) of the broad envelope containing the 625 cm^{-1} band, plotted on a common

y-axis versus the electrode potential during voltammetric oxidation (Figure 4A) and the ensuing reduction (Figure 4B). The former quantity is obtained from the potential-dependent faradaic charge contained under the background-corrected voltammetric waves, assuming that each ML corresponds to 280 μC cm^{-2}. (This value refers to a one-electron process occurring on hexagonally close-packed copper). The integrated SERS intensities are normalized to their maximum values.

It is evident from Figure 4A that the SERS intensities "lead" the Cu_2O growth process; although having an essentially common onset potential, −0.48 V, the former response becomes almost invariant for oxide thickness greater than about 15−20 ML. Figure 4B illustrates a related, albeit less marked, disparity in that during cathodic oxide removal the SERS response "lags" somewhat the corresponding decrease in oxide thickness. No significant attenuation of SERS intensity is observed until the oxide thickness is reduced somewhat (ca. 20−25%) below its maximum value.

These findings can be understood on the basis of the anticipated spatial properties of SERS, given that the production of a thickening (and presumably largely uniform) Cu_2O film will inevitably lead to the presence of metal−oxide vibrations that are increasingly separated spatially from the reduced copper moieties that are presumably responsible for SERS (cf., nickel oxide films[10b]). Therefore, as the oxide film grows thicker than the characteristic distances over which the SERS effect propagates, a saturation of SERS intensity is expected, in harmony with the observations (Figure 4). The effective "separation distance" over which SERS apparently extends on the basis of Figure 4A, ca. 15−20 ML (∼ 30−40 Å), is roughly consistent with theoretical and experimental estimates.[16] An additional experiment was performed in which a thicker (ca. 200 ML) Cu_2O film was grown by oxidizing copper in 0.1 M NaOH + 0.1 M $NaClO_4$ at −0.25 V for 20 min. The SERS intensity observed for this markedly thicker oxide layer, however, is again similar to that obtained for the 20 ML film. In addition to supporting the above interpretation, this suggests that the absorption of the incident laser light is insignificant (at least for the oxide thickness considered here); otherwise the signal would decrease with increasing oxide thickness and a SERS intensity maximum (instead of a plateau) obtained.[10b]

The spatial mechanism for electrochemical removal of the Cu_2O film depends largely on physical properties such as resistivity, porosity, and uniformity. The present analysis suggests a simple model for this process. The similarity of SERS intensity−oxide thickness correlations evident in Figure 4A,B suggests that the reduction probably occurs via a spatial mechanism which is roughly the microscopic reverse of the oxidation. This implies that the reduction process is initiated within the oxide film primarily at the metal/oxide rather than the oxide−solution interface, and proceeds outward. This is because SERS will still "see" an oxide film extending at least 30−40 Å away from the Cu/Cu_2O interface even after film reduction has commenced, thereby accounting for the "lag" in the initial attenuation of the band intensity relative to the Coulombic data (Figure 4B). Such a mechanism will occur if the mobility of ions is higher than that of electrons through the oxide film.

Irrespective of such details of the oxide growth/removal mechanism, it is noteworthy that the potential-dependent appearance of a surface oxide in alkaline solution as deduced in concordant fashion by SERS and voltammetric measurements (Figure 4) coincides with the thermodynamics of bulk-phase Cu_2O formation. The reason is to found in the multilayer nature of the films, so that the oxide experiences largely a uniform solid-state, rather than a solid−liquid interfacial, environment. Nonetheless, it is very likely that monolayer (and/or submonolayer) levels of oxide/hydroxide species are also present on copper in alkaline media at potentials negative of those corresponding to Cu_2O film production. Such species would be stabilized by bonding to the metallic copper surface and therefore can be present over wide, more negative, potential ranges. (As is generally true for oxygenated and other electron-rich adsorbates, altering the potential negative will eventually trigger desorption. Such potential-dependent equilibria are commonly observed both for anionic species and those featuring adsorbate−metal charge transfer.)

Evidence for the occurrence of oxide/hydroxide adsorption on copper in alkaline media is available not only from conventional electrochemical data[17] but also, as already mentioned, from SERS on Cu(111).[4] The latter entails the observation of Raman bands at ca. 700 and 3500 cm^{-1}, assigned to metal(hollow site)−OH and O−H vibrations, respectively.[4] The increasing intensity of these bands toward more *negative* potentials (down to −1.3 V), together with their sluggish formation rates, led to the suggestion that a CuOH species is formed by reduction/protonation of subsurface oxygen present at higher potentials.[4] While this SER spectral behavior was not observed in the present work, this could be due to the very low intensity of the 700 cm^{-1} band as well as differences in surface state. (Note that long integration times and potential-difference spectral tactics, along with a more sensitive Raman spectrometer, were utilized in ref 4.) Nevertheless, the 800 and 460 cm^{-1} features seen here in alkaline solution at negative potentials, especially after Cu_2O film removal (Figure 2, vide supra), may well arise from similar surface chemistry.

Neutral Media: Effect of Chloride on Surface Oxidation. We now describe corresponding potential-dependent SERS data for copper in neutral media for comparison with the results obtained in alkaline solution. Figure 5A displays potential-dependent SER spectra obtained for copper subjected to electrochemical oxidation and subsequent reduction in 0.1 M $NaClO_4$ (pH 6). Stepwise potential alterations were applied and the spectra obtained at the indicated potentials, starting at −0.8 V (bottom spectrum). It is apparent from Figure 5A that surface oxidation occurs at −0.2 V during the positive-going potential sequence, in that a broad asymmetric SERS band appears at ca. 620 cm^{-1}. This potential-dependent behavior is consistent with the Pourbaix diagram which yields a value of $E°_{(Cu_2O)}$ equal to −0.2 V at pH 6.[13] This broad SERS feature, reminiscent of the 625/525 cm^{-1} bands obtained in alkaline electrolytes (although lacking a resolved lower-frequency component), is therefore again assigned to Cu_2O. The unbuffered nature of the neutral pH electrolyte, however, precluded a detailed potential-dependent analysis of the spectra.

It is also of interest to examine the influence of a strongly complexing anion, such as chloride, on the SER spectra in order to ascertain the possible effects of competitive chloride/oxide phase-film formation on the surface chemistry. The neutral pH condition is interesting in this regard since the Pourbaix diagram suggests then a fine balance between the alternative potential-dependent formation of Cu(I) oxide and chloride phase films.[13,18] The experiments were performed in 0.1 M KCl solution (pH 6); resulting potential-dependent SER spectra are shown in Figure 5B. During the positive-going potential excursion, copper was oxidized to Cu_2O at least by −0.2 V as signaled again by the appearance of the 500−625 cm^{-1} features. An additional, sharper, SERS band is evident at 290 cm^{-1} upon further

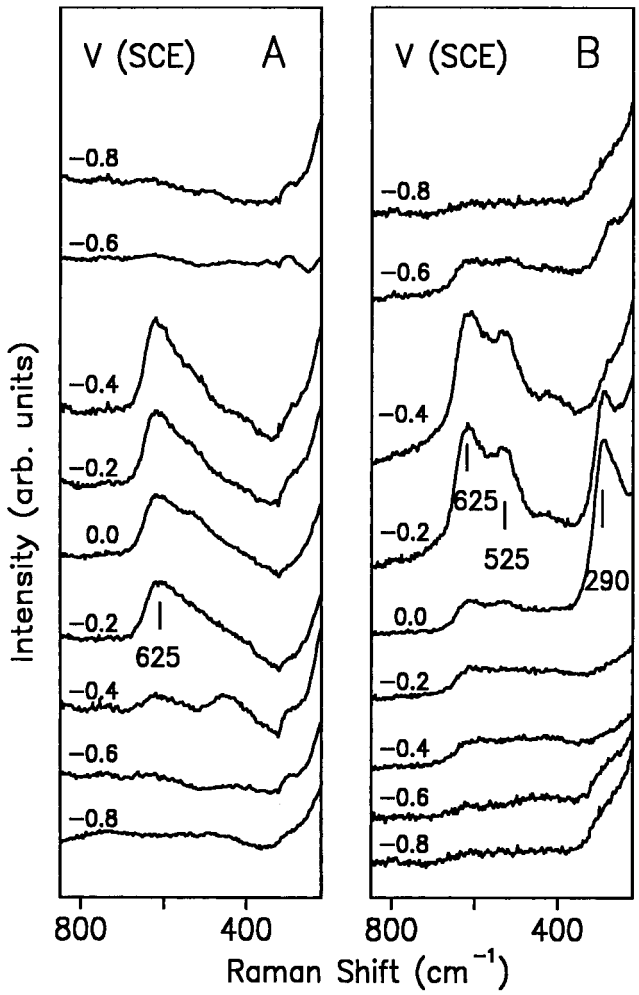

Figure 5. Potential-dependent SER spectra obtained for electrochemical oxidation and subsequent reduction of copper in (A) 0.1 M $NaClO_4$ and (B) 0.1 M KCl, starting from − 0.8 V (bottom spectra). The spectral integration time was 20 s.

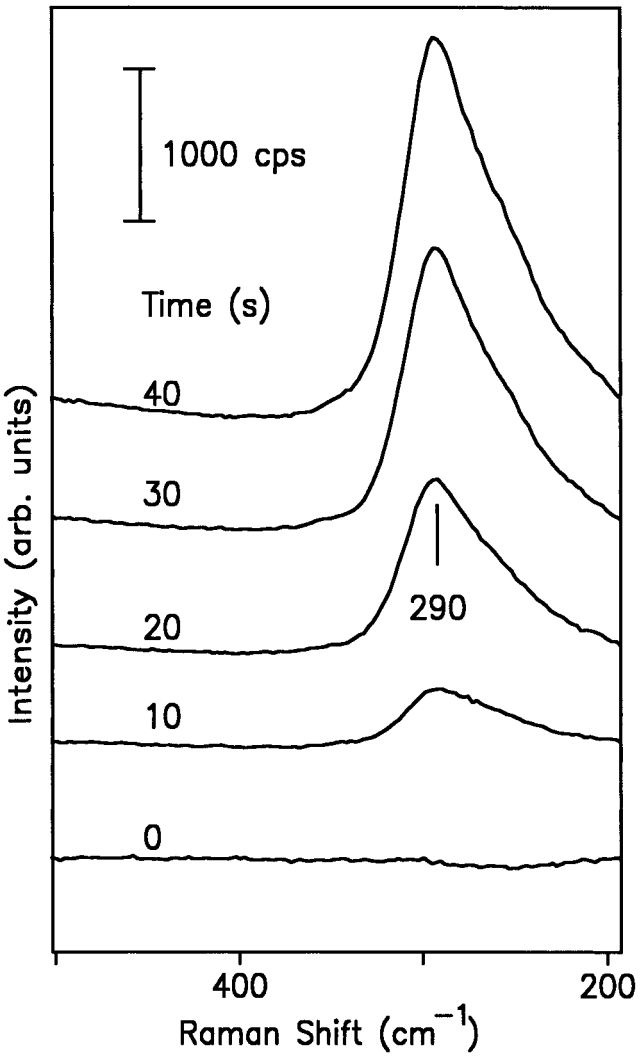

Figure 6. Time-dependent SER spectra for copper in 0.1 M KCl immediately following a potential step from −0.8 to 0 V. The spectral integration time was 1 s. The cps scale shown refers to photon counts per second.

increasing the potential to 0 V which does not appear in the absence of chloride (Figure 5A). This strongly suggests that the 290 cm^{-1} feature arises from a Cu−Cl stretching mode of adsorbed chloride or copper chloride phase film. For comparison, values of the metal−Cl stretches on gold,[19] silver,[19] and copper[20] have been reported to be 260, 240, and 290 cm^{-1}, respectively, at 0 V.

Cyclic voltammograms of copper in 0.1 M KCl (not shown) indicate the onset of metal dissolution at −0.1 V. Figure 6 shows time-dependent SER spectra for copper in 0.1 M KCl immediately following a potential step from −0.8 to 0 V. The 290 cm^{-1} band intensity increases continuously with time for the first 60 s or so. The finding suggests that a CuCl film, rather than adsorbed chloride, is formed at 0 V that can grow "continuously", presumably due to a porous structure which allows chloride ions to readily reach the underlying metal and facilitate further corrosion. This contrasts with the more "self-limiting" growth displayed by the aforementioned Cu_2O, presumably since its more compact structure acts as a passivating layer against corrosion in alkaline solution. Noteworthy is the very high intensity of the Cu−Cl SERS feature under these conditions (Figure 6), which reaches peak amplitudes that are typically 20−50-fold larger than for the metal−oxygen stretching bands considered here.

Ex-situ XPS experiments were also undertaken to facilitate the assignment of the 290 cm^{-1} SERS feature, exploiting the elemental and oxidation-state specificity of this technique. To forge a reliable link between the in-situ SERS and this ex-situ characterization, however, it is critical to ensure that the surface speciation is not modified upon emersion. This question was initially addressed by examining the SER spectra in air after emersion from 0.1 M KCl at 0 V and rinsing with water. The spectrum displayed the same 290 cm^{-1} feature as seen in the in-situ electrochemical cell, indicative of the stability of this species upon emersion, along with its identification as a surface species rather than a dissolved counterpart.

In view of the presence of the 290 cm^{-1} SERS band at 0 V but not at −0.8 V (Figure 5B), a pair of copper samples were examined by XPS which were emersed similarly at 0 and −0.8 V in 0.1 M KCl solution, the latter serving as a control experiment. The results show the presence of a Cl 2p doublet in the spectrum obtained from the former but not in the latter condition, confirming that the 290 cm^{-1} SERS band arises from chloride species rather than oxide. The binding energies of the Cl 2p doublets are 198.8 and 200.4 eV, while the Cu $2p_{3/2}$ peak appears at 932.7 eV. For comparison, the literature XPS spectrum of bulk CuCl contains Cl 2p peaks at 198.8 and 200.5 eV along with Cu $2p_{3/2}$ peak at 932.7 eV, while that of bulk $CuCl_2$ exhibits the former transitions at 199.1 and 200.7 eV with the latter at 935.7 eV.[21] The 290 cm^{-1} SERS feature at 0

V can therefore be assigned predominately to a CuCl phase film formed during metal dissolution, rather than to a $CuCl_2$ film or to adsorbed chloride ions, even though the latter may contribute to the Raman band (vide infra).

It is worthwhile to consider further the competitive potential-dependent formation of Cu(I) oxide and chloride phase films as gleaned from the potential-dependent SER spectra. Figure 5B shows that in neutral chloride solution Cu_2O formation is favored at lower potentials, particularly during the return (negative-going) excursion where the 625/525 cm^{-1} doublet is well-resolved, but is replaced by CuCl formation at 0 V. This potential-dependent transition is significant, since it is *not* expected from the Pourbaix diagram of the $Cu-H_2O-Cl^-$ system which shows that the thermodynamics of Cu_2O versus CuCl formation depends *only* on the pH and Cl^- concentration.[13,18] Specifically, in 0.1 M Cl^- solution, $CuCl_2^-$ is produced via reaction 2a, along with its precipitation to form a CuCl phase film (reaction 2b):

$$Cu + 2Cl^- \rightarrow CuCl_2^- + e^- \qquad (2a)$$

$$CuCl_2^- \rightarrow CuCl + Cl^- \qquad (2b)$$

At pH values above 5, however, Cu_2O rather than CuCl should be formed upon oxidation, as a result of the equilibrium (reaction 3):

$$Cu_2O + 2H^+ + 2Cl^- \leftrightarrow 2CuCl + H_2O \qquad (3)$$

Consequently, then, positive-going potential excursions at a given pH should yield a pure CuCl or Cu_2O phase film, the latter being formed at pH > 5.

This apparent contradiction between the potential-dependent SER spectra and the thermodynamic expectations is not in itself discomforting since the extent of phase film formation is affected markedly by kinetics, and the films themselves are very thin (probably a few monolayers) so to bring into play surface rather than purely bulk-phase phenomena. The experimental observation of successive potential-induced Cu_2O and then CuCl formation (Figure 5B) can be accounted for by the occurrence of a kinetic limitation to Cu_2O film growth, together with the occurrence of Cl^- migration through the film to access the underlying copper substrate. The formation of CuCl via reactions 2a and 2b is thermodynamically favorable in 0.1 M chloride above the standard equilibrium potential $E°_{(CuCl)} = -0.05$ V vs SCE.[13]

The potential-dependent CuCl formation was further explored by similar SER spectra obtained in *alkaline* chloride solution (0.1 M KCl + 0.1 M NaOH). The results are essentially the same as those shown in Figure 2A,B, obtained in chloride-free solution, showing the dominant presence of Cu_2O without any evidence of CuCl formation (or Cl^- adsorption) at potentials as high as 0.3 V. This observation, however, does not contradict the above interpretation since the equilibrium potential for Cu_2O formation at pH 13, $E°_{(Cu_2O)} = -0.54$ V, is markedly more negative than that for CuCl production. This factor together with the more facile Cu_2O kinetics in alkaline solution will yield a thicker oxide before reaching $E°_{(CuCl)}$, −0.05 V, thereby hindering Cl^- migration through the film to form CuCl.

Acidic Media. So far, we have examined copper surfaces at sufficiently high pH values, ≥6, so that anodic Cu_2O formation occurs at potentials below where metal dissolution to Cu^{2+} ions proceeds. There is much interest, however, in scrutinizing copper surface chemistry in noncomplexing acidic media.[11,22,23] Under these conditions, oxide phase films should be absent, facilitating the identification of potential-dependent adsorption of oxygenated species also formed by water decomposition. In particular, Gewirth and co-workers have observed by in situ AFM the apparent growth of ordered oxygen (or oxygen-like) chains on Cu(100) and (110) in perchloric acid and sulfuric acid electrolytes.[11] Interestingly, such real-space adlayer patterns are similar to those observed upon oxygen adsorption on Cu(110) in UHV.[24] Unlike the oxide formed at higher pH values (vide supra), such species are inherently adsorbates rather than constituting the initial stages of eventual bulk-phase oxidation since production of the former, but not the latter, occurs at markedly lower potentials than predicted by the Pourbaix diagram.

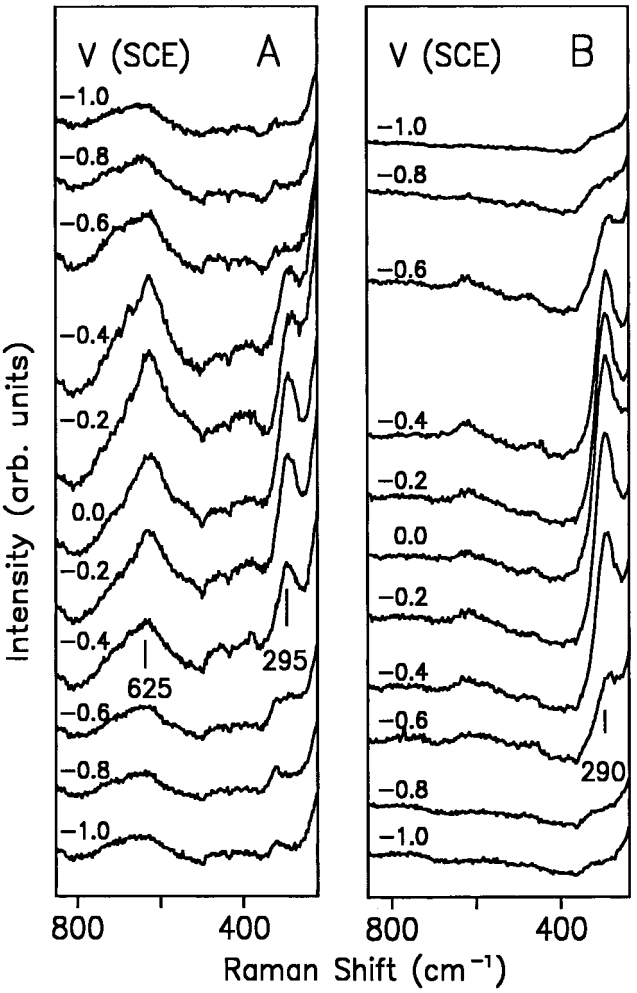

Figure 7. SER spectra obtained on copper for initially positive- and then negative-going potential sequence, from −1.0 V (bottom spectrum) to 0 V and return, in (A) 0.1 M H_2SO_4 and (B) 0.1 M H_2SO_4 + 0.1 M KCl. The spectral integration time was 40 s.

Figure 7A shows a potential-dependent sequence of SER spectra obtained for copper in 0.1 M H_2SO_4, again starting at a negative potential, −1.0 V, in the (upward-stacked) sequence shown up to 0 V and return, the spectral acquisition being 20 s each time. Sulfuric acid was utilized since perchloric acid (and perchlorates) are more susceptible to chloride contamination (including Cl^- formation by ClO_4^- reduction). Nevertheless, Figure 7A shows a weak band appearing at 290−295 cm^{-1} for potentials above −0.4 V, attributable to adsorbed chloride. As expected, the deliberate addition of Cl^- to the electrolyte yields a marked intensity enhancement of this vibrational feature (Figure 7B). Unlike the CuCl phase film noted above (Figure 6), the ca. 290 cm^{-1} band observed at potentials negative of 0 V does not grow with time when initiated by a positive-going

potential step. This observation, together with the slight (5 cm^{-1}) increase in the peak frequency from −0.6 to −0.2 V, supports further its assignment to adsorbed chloride rather than a CuCl phase film.

More intriguingly, however, a broad yet clearly discernible band peaked at 625 cm^{-1} appears on copper in 0.1 M H_2SO_4 by −0.4 V during the positive-going potential excursion. The band intensity is maintained up to the positive limit, 0 V, and decreases again only upon lowering the potential to −0.6 V (Figure 7A). Significantly, the 625 cm^{-1} band intensity is potential independent even in the region, above −0.1 up to 0.1 V, where copper anodic dissolution proceeds. Essentially the same potential-dependent spectral behavior was obtained in 0.1 M $HClO_4$, although the 295 cm^{-1} band tended to be more pronounced in this medium. This latter finding eliminates the possibility that the 625 cm^{-1} band arises from adsorbed electrolyte anions, especially since sulfate should be more strongly bound than perchlorate. While sulfate SERS features have apparently been observed on copper,[25] a much higher (2 M) sulfuric acid concentration was utilized in ref 25 than here. Substitution of H_2O by D_2O solvent yielded no discernible isotopic shift in the 625 cm^{-1} band frequency, similar to the Cu_2O film (vide supra). Although the breadth and nonsymmetric nature of the band hampered such measurements, the results support its assignment to a Cu−O rather than a Cu−OH type of vibration. Note that metal−oxygen stretch vibrations for both adsorbed oxygen and oxide are commonly located in the 500−700 cm^{-1} frequency region.[5,7,8]

The potential-dependent stability of the 625 cm^{-1} feature in Figure 7A is also consistent with an adsorbed oxygen moiety. The ca. 1 V lower potential required to form the adsorbate relative to bulk-phase Cu_2O in acidic media implies the presence of a substantial (ca. 20 kcal mol^{-1}) bond energy contribution arising purely from surface stabilization (cf., metal underpotential deposition). This energy stabilization is indicative of the presence of oxygen bound to surface sites consisting of reduced copper atoms or, alternatively, to a Cu−O layer featuring at least partial metal−oxygen place exchange. (These two states of interfacial oxygen are often referred to as "adsorbed oxygen" and "oxide", respectively. They are both distinct from, although may be mechanistic precursors to, the formation of multilayer and ultimately bulk-phase metal oxide films.) Nonetheless, the appearance (and frequency) of the "anomalous oxygen" 625 cm^{-1} feature is not greatly different from that for Cu_2O films. This point is illustrated in Figure 8, showing examples of SER spectra obtained on copper in four electrolytes, as indicated, each at −0.2 V. [Note that while the relative Raman intensity scales for the different media have been altered somewhat for pictorial convenience, the peak intensities of each of the ca. 600−650 cm^{-1} bands in Figure 8 (taken versus the continuum background) are actually within 2−3-fold of each other.]

Analogously to the AFM results, yet in a complementary (and more chemically specific) fashion, then, the appearance of the ca. 625 cm^{-1} band provides direct evidence for the presence of an oxygen adsorbate on copper *virtually throughout* the polarizable electrode potential region in acidic electrolytes (0.1 M H_2SO_4 and $HClO_4$), lying between the onset of cathodic hydrogen evolution and anodic metal dissolution, ca. −0.7 to −0.1 V, respectively. Beside the origin of this anomalous adsorbate, O_{ads}, these results together raise the interesting issue of the reasons for its near-ubiquitous presence in acidic media, contrasting its apparent absence in neutral and alkaline electrolytes. At least part of the answer to this perplexing question may be found in competitive adsorption. The effect is apparent in Figure 7, in

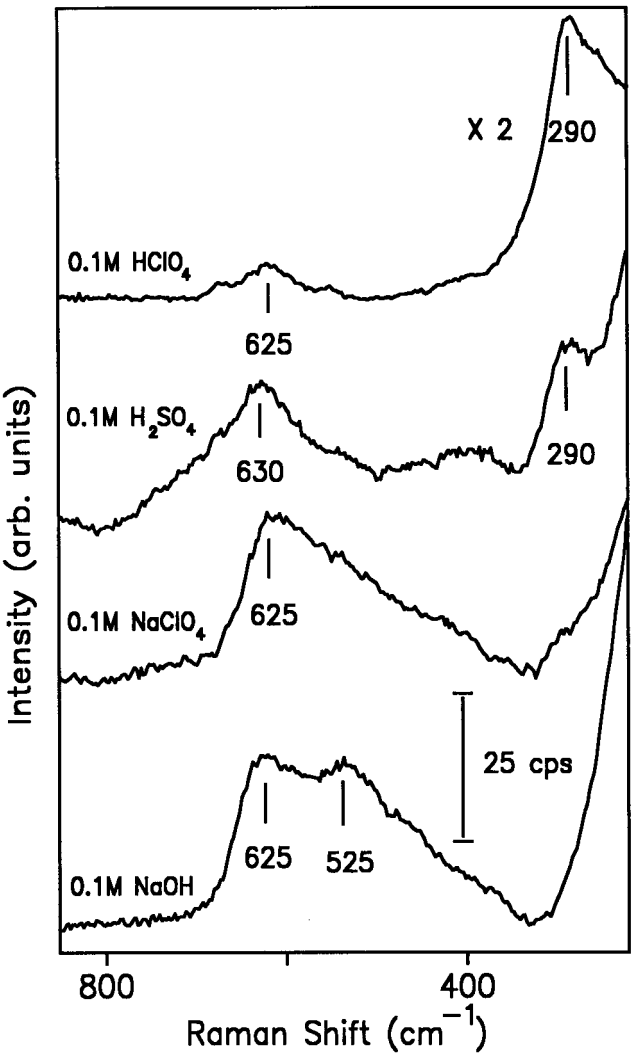

Figure 8. Selected SER spectra obtained for copper in different electrolytes, as indicated, at −0.2 V vs SCE (during positive-going potential excursion). The cps scale shown refers to photon counts per second.

that the addition of chloride to the 0.1M H_2SO_4 (Figure 7B) is seen to virtually eliminate the 625 cm^{-1} band, being replaced within the same potential range (−0.6 to 0 V) by the Cu−Cl stretch due to adsorbed chloride and/or a CuCl phase film.

More generally, O_{ads} may well be prevalent only in acidic media because different oxygenated species are present instead in higher pH electrolytes. Perhaps the simplest, as well as most viable, explanation is to invoke the presence of adsorbed OH and/or oxide (along with Cu_2O formation at more positive potentials) at higher pH values that inhibit the formation of O_{ads}. This notion is supported not only by the aforementioned spectral as well as electrochemical evidence for adsorbed hydroxyl (or hydroxide), OH_{ads}, in alkaline electrolytes,[4,17] but also by the expectation that O_{ads} should be favored increasingly versus OH_{ads} in acidic media, where the OH^- activities become vanishingly small. Nonetheless, the adsorbed "oxygen chains" inferred to grow on the basis of in-situ AFM images on Cu(100) and (110) in similar acidic media, and within the same electrode potential range as the O_{ads} species deduced from the SERS data on polycrystalline Cu, suggest strongly that the latter moiety also involves some degree of adsorbate ordering. Such a deduction suggests at least two further notions. First, the nucleation/growth processes associated with the formation of ordered O_{ads} could be sluggish and inhibited readily (or even halted) by the presence

of coadsorbates, especially oxide species which will disrupt the surface lattice. The slow, electrochemically irreversible, nature of oxygen adsorption on copper in acidified perchlorate is indeed supported by pH-dependent electrochemical measurements.[22b] Second, such ordered O_{ads} structures may be stabilized in acidic media by hydrogen bonding with hydronium ions, especially if the adsorbate carries a partial negative charge. Both these possibilities, although speculative, constitute potential additional factors favoring the substantial presence of O_{ads} only in acidic aqueous electrolytes with "noncomplexing" anions.

Concluding Remarks

Regardless of the structural details, the present SERS results show clearly that the copper surface in acidic as well as alkaline noncomplexing aqueous media conspires to acquire an oxygenated layer of some form, whether it be adsorbed oxygen atoms, adsorbed OH/OH^-, an oxide/hydroxide film, or a multilayer (bulk-phase) oxide, over wide electrode potential ranges, typically ca. −0.8 to 0 V vs SCE. This spans most of the potential region, lying between copper anodic dissolution and cathodic hydrogen evolution, that might be expected to constitute the "polarizable double-layer" range in conventional electrochemical terms. As on a number of other reactive metals, including the relatively noble Pt-group surfaces, however, the presence of a strict double-layer region, where the inner layer consists of adsorbed water rather than chemisorbed H_2O decomposition products over a significant potential range, is doubtful on copper. The underlying fundamental reason for this situation clearly lies in the very high affinity of copper for oxygen, although, unlike early transition metals, the adsorbed oxygen/oxide species can be formed and removed readily by suitable electrode-potential excursions. The high affinity of copper also for chlorine[26] complicates as well as enriches the surface chemistry, especially since Cl^- trace contaminants are common in aqueous electrolytes. The adsorptive electrochemistry of copper may therefore often feature competitive adsorption of chlorine and oxygen species, which extend to the formation of corroding versus stable phase films at higher potentials. However, the ability of SERS to readily distinguish between chlorine and oxygen species from their different metal−adsorbate stretching frequencies (arising partly from the differing atomic masses as well as force constants[5]) provides a valuable adsorbate diagnosis in this regard.

The complex nature of copper−aqueous surface electrochemistry is, of course, responsible for the continued uncertainty and the somewhat suggestive, rather than conclusive, interpretations of adsorbate speciation and potential-dependent stability that abound even in the recent literature. Despite the inevitable limitations of SERS, the present results are nonetheless considered to shed new light on the surface speciation. A related study, demonstrating the utility of SERS for elucidating oxygen−copper surface chemistry in ambient gaseous environments, and specifically an ability to alter the copper−gaseous surface state by controlled pH rinsing, will be reported elsewhere.[27] More generally, the burgeoning as well as diverse practical importance of copper as a material in, for example, microelectronics as well as heterogeneous catalysis, provides a persuasive reason to strive for a more complete understanding of its surface chemistry, especially in ambient water/oxygen environments.

Acknowledgment. This work was supported by the National Science Foundation, via grants from the Chemical and Transport Division (to C.G.T. and M.J.W.) and the Analytical and Surface Chemistry Division (to M.J.W.).

References and Notes

(1) (a) Kautek, W.; Gordon, J. G., II. *J. Electrochem. Soc.* **1990**, *137*, 2672. (b) Feng, Y.; Siow, K.-S.; Teo, W.-K.; Tan, K.-L.; Hsieh, A.-K. *Corrosion* **1997**, *53*, 389.

(2) (a) Hamilton, J. C.; Farmer, J. C.; Anderson, R. J. *J. Electrochem. Soc.* **1986**, *133*, 739. (b) Mayer, S. T.; Muller, R. H. *J. Electrochem. Soc.* **1992**, *139*, 426.

(3) Melendres, C. A.; Bowmaker, G. A.; Leger, J. M.; Beden, B. *J. Electroanal. Chem.* **1998**, *449*, 215.

(4) Härtinger, S.; Pettinger, B.; Doblhofer, K. *J. Electroanal. Chem.* **1995**, *397*, 335.

(5) Desilvestro, J.; Weaver, M. J. *J. Electroanal. Chem.* **1986**, *209*, 377.

(6) (a) Leung, L.-W. H.; Weaver, M. J. *J. Am. Chem. Soc.* **1987**, *109*, 5113. (b) Leung, L.-W. H.; Weaver, M. J. *Langmuir* **1988**, *4*, 1076.

(7) Zhang, Y.; Gao, X.; Weaver, M. J. *J. Phys. Chem.* **1993**, *97*, 8656.

(8) (a) Tolia, A. A.; Smiley, R. J.; Delgass, W. N.; Takoudis, C. G.; Weaver, M. J. *J. Catal.* **1994**, *150*, 56. (b) Williams, C. T.; Tolia, A. A.; Chan, H. Y. H.; Takoudis, C. G.; Weaver, M. J. *J. Catal.* **1996**, *163*, 63. (c) Chan, H. Y. H.; Williams, C. T.; Weaver, M. J.; Takoudis, C. G. *J. Catal.* **1998**, *174*, 191. (d) Chan, H. Y. H.; Takoudis, C. G.; Weaver, M. J. *J. Catal.* **1997**, *172*, 336. (e) Williams, C. T.; Chen, E. K.-Y.; Takoudis, C. G.; Weaver, M. J. *J. Phys. Chem. B* **1998**, *102*, 4785.

(9) Zou, S.; Weaver, M. J. *Anal. Chem.* **1998**, *70*, 2387.

(10) (a) Desilvestro, J.; Corrigan, D. A.; Weaver, M. J. *J. Electrochem. Soc.* **1988**, *135*, 885. (b) Gosztola, D.; Weaver, M. J. *Langmuir* **1989**, *5*, 776.

(11) (a) Cruickshank, B. J.; Sneddon, D. D.; Gewirth, A. A. *Surf. Sci.* **1993**, *281*, L308. (b) LaGraff, J. R.; Gewirth, A. A. *Surf. Sci.* **1995**, *326*, L461.

(12) Wilke, T.; Gao, X.; Takoudis, C. G.; Weaver, M. J. *J. Catal.* **1991**, *130*, 62.

(13) Bertocci, U.; Turner, D. R. *Encyclopedia of Electrochemistry of the Elements*, Vol. II; Bard, A. J., Ed.; Marcel Dekker: New York, 1974; p 383−497.

(14) Chang, R. K.; Laube, B. L. *CRC Crit. Rev. Solid State Mater. Sci.* **1984**, *12*, 1.

(15) Sueyoshi, T.; Sasaki, T.; Iwasawa, Y. *J. Phys. Chem. B* **1997**, *101*, 4648.

(16) (a) Cotton, T. M.; Uphaus, R. A.; Mobius, D. *J. Phys. Chem.* **1986**, *90*, 6071. (b) Ye, Q.; Fang, J.; Sun, L. *J. Phys. Chem. B* **1997**, *101*, 8221. (c) Campion, A.; Kambhampati, P. *Chem. Soc. Rev.* **1998**, *27*, 241.

(17) (a) Härtinger, S.; Doblhofer, K. *J. Electroanal. Chem.* **1995**, *380*, 185. (b) Droog, J. M. M.; Alderliesten, C. A.; Alderliesten, P. T.; Bootsma, G. A. *J. Electroanal. Chem.* **1980**, *111*, 61. (c) Droog, J. M. M.; Schlenter, B. *J. Electroanal. Chem.* **1980**, *112*, 387. (d) For a recent review, see: Marichev, V. A. *Electrochim. Acta* **1998**, *43*, 2203.

(18) Tromans, D.; Sun, R.-H. *J. Electrochem. Soc.* **1991**, *138*, 3235.

(19) (a) Gao, P.; Weaver, M. J. *J. Phys. Chem.* **1986**, *90*, 4057. (b) Leung, L.-W. H.; Gosztola, D.; Weaver, M. J. *Langmuir* **1987**, *3*, 45.

(20) (a) Niaura, G.; Malinauskas, A. *Chem. Phys. Lett.* **1993**, *207*, 455. (b) Brown, G. M.; Hope, G. A. *J. Electroanal. Chem.* **1996**, *405*, 211. (c) El'tsov, K. N.; Zueva, G. Y.; Klimov, A. N.; Martynov, V. V.; Prokhorov, A. M. *Chem. Phys. Lett.* **1989**, *158*, 271.

(21) Sesselmann, W.; Chuang, T. J. *Surf. Sci.* **1986**, *176*, 32.

(22) (a) Siegenthaler, H.; Jüttner, K. *J. Electroanal. Chem.* **1984**, *163*, 327. (b) Vilche, J. R.; Jüttner, K. *Electrochim. Acta* **1987**, *32*, 1567.

(23) (a) Bradley, R. A.; Friedrich, K. A.; Wong, E. K. L.; Richmond, G. L. *J. Electroanal. Chem.* **1991**, *309*, 319. (b) Wong, E. K. L.; Friedrich, K. A.; Robinson, J. M.; Bradley, R. A.; Richmond, G. L. *J. Vac. Sci. Technol. A* **1992**, *10*, 2985.

(24) For example: (a) Coulman, D. J.; Wintterlin, J.; Behm, R. J.; Ertl, G. *Phys. Rev. Lett.* **1990**, *64*, 1761. (b) Chua, F. M.; Kuk, Y.; Silverman, P. J. *Phys. Rev. Lett.* **1989**, *63*, 386.

(25) Brown, G. M.; Hope, G. A. *J. Electroanal. Chem.* **1995**, *382*, 179.

(26) (a) Ehlers, C. B.; Villegas, I.; Stickney, J. L. *J. Electroanal. Chem.* **1990**, *284*, 403. (b) Stickney, J. L.; Ehlers, C. B.; Gregory, B. W. *Langmuir* **1988**, *4*, 1368.

(27) Chan, H. Y. H.; Takoudis, C. G.; Weaver, M. J. *Electrochem. Solid State Lett.*, in press.